Journal of Enzyme Inhibition and Medicinal Chemistry

ISSN: 1475-6366 (Print) 1475-6374 (Online) Journal homepage: http://www.tandfonline.com/loi/ienz20

Design, synthesis and biological activity of 1H-indene-2-carboxamides as multi-targeted anti-Alzheimer agents

Mehmet Koca, Kadir Ozden Yerdelen, Baris Anil, Zeynep Kasap, Handan Sevindik, Ibrahim Ozyurek, Gulsen Gunesacar & Kubra Turkaydin

To cite this article: Mehmet Koca, Kadir Ozden Yerdelen, Baris Anil, Zeynep Kasap, Handan Sevindik, Ibrahim Ozyurek, Gulsen Gunesacar & Kubra Turkaydin (2016): Design, synthesis and biological activity of 1H-indene-2-carboxamides as multi-targeted anti-Alzheimer agents, Journal of Enzyme Inhibition and Medicinal Chemistry, DOI: 10.1080/14756366.2016.1186019

To link to this article: http://dx.doi.org/10.1080/14756366.2016.1186019

Journal of Enzyme Inhibition and Medicinal Chemistry

www.tandfonline.com/ienz
ISSN: 1475-6366 (print), 1475-6374 (electronic)

J Enzyme Inhib Med Chem, Early Online: 1–11
 DOI: 10.1080/14756366.2016.1186019

Taylor & Francis
Taylor & Francis Group

RESEARCH ARTICLE

Design, synthesis and biological activity of 1H-indene-2-carboxamides as multi-targeted anti-Alzheimer agents

Mehmet Koca[1], Kadir Ozden Yerdelen[1], Baris Anil[2], Zeynep Kasap[1], Handan Sevindik[3], Ibrahim Ozyurek[2], Gulsen Gunesacar[1], and Kubra Turkaydin[1]

[1]Department of Pharmaceutical Chemistry, [2]Department of Organic Chemistry, and [3]Department of Pharmacognosy, Ataturk University, Erzurum, Turkey

Abstract

The aim of this study was to design new molecules and evaluate their anticholinesterase and amyloid beta ($A\beta_{1-42}$) inhibition activities as multifunctional drug candidates for the treatment of Alzheimer's disease (AD). A series of 5,6-dimethoxy-1H-indene-2-carboxamides (**1**–**22**) was synthesized; cholinesterase inhibitory activities of the compounds were measured according to Ellman's colorimetric assay, while the thioflavin T assay was used for measuring the inhibition of $A\beta_{1-42}$ aggregation. The results revealed that most compounds showed higher inhibitory activity against BuChE than AChE. Compounds **20** and **21** were found to be the most potent BuChE inhibitors with respective IC_{50} values of 1.08 and 1.09 μM. Compounds **16**, **20**, **21** and **22** exhibited remarkable inhibition of $A\beta_{1-42}$ aggregation. Kinetic analysis showed that the most potent BuChE inhibitor (**20**) acted as a noncompetitive inhibitor. Docking studies suggested that inhibitor **20** displayed many potential hydrogen-bondings with the PAS of BuChE. These results suggest that compound **20** may be an especially promising multifunctional drug for the prevention and treatment of AD.

Keywords

AChE, Alzheimer, Aβ1–42, BuChE, molecular modeling

History

Received 3 March 2016
Revised 28 March 2016
Accepted 30 March 2016
Published online 23 May 2016

Introduction

Alzheimer's disease (AD), which is a type of mental health decline or dementia, is a complex neurodegenerative disorder with highest prevalence in the elderly population. Causes of and effective treatments for this disease remain uncertain, requiring complex attempts to develop new, effective anti-AD drugs. In recent years, the most popular pathophysiological approaches have suggested that AD is characterized by low levels of acetylcholine (ACh), increased oxidative stress, high levels of some metal ions, and overproduction and aggregation of $A\beta$[1–3]. The oldest and most popular current strategy for AD treatment is based on the cholinergic hypothesis and specifically on acetylcholinesterase (AChE) inhibition to improve cholinergic neurotransmission in the brain by increasing the levels of ACh[4–6]. AChE's sister enzyme, butyrylcholinesterase (BuChE), has also been found to be capable of compensating for the missing AChE catalytic functions in the synaptic cleft[7,8]. This function has driven increased attention on BuChE, due to its ability to hydrolyze ACh and other esters. Inhibition of both cholinesterase enzymes (ChEs) should provide additional contributions in the treatment of AD[9–11].

The second main therapeutic strategy for AD is based on preventing Aβ aggregation. According to this amyloid hypothesis, aggregation of amyloid peptide is a critical stage in AD development; accumulation of the Aβ peptide in neurons may induce biochemical events leading to neuronal dysfunctions[12]. In addition, recent studies have shown that oxidative damage may increase the incidence of amyloid plaques in the brains of AD patients[13]. Another hypothesis, known as the metal hypothesis, indicates that high levels of metal ions (Fe^{2+}, Cu^{2+} and Zn^{2+}) cause severe and fatal neurologic disorders. The accumulation of metal ions is closely associated with abnormal clumps of Aβ plaques that are a hallmark of AD[13–16]. Several AChE inhibitors such as donepezil, galantamine, and rivastigmine have been used for the treatment of AD[17]. Among these drugs, donepezil was approved for the treatment of mild to moderate dementia in AD by the United States Food and Drug Administration in 2006[18]. Many studies have demonstrated that donepezil analogues (**I** and **II**) are able to interact with the catalytic anionic site (CAS) and the peripheral anionic site (PAS) of AChE, with their highest inhibitory activities at nanomolar concentrations (Figure 1)[3]. In our recent docking studies work, we have synthesized a series of tertiary diamide (2-butendiamide and ethanediamide) derivatives and described their possible hydrogen-bonding interactions with the –C=O and –NH groups between the amide functional group and both active sites of AChE[19–23]. The positive contributions on cholinesterase inhibition activity of halogenated (F, Cl and Br) phenyl rings have also been investigated in these studies.

In this study, the 5,6-dimethoxyindanone structure of donepezil, which is the structural part responsible for binding AChE to the PAS, was taken as the main structural moiety to design new

Address for correspondence: Kadir Ozden Yerdelen, Assist. Prof., Department of Pharmaceutical Chemistry, Faculty of Pharmacy, Ataturk University, 25240 Erzurum, Turkey. Tel: +90 4422315220. Fax: +90 4422360962. E-mail: dadasozden@gmail.com

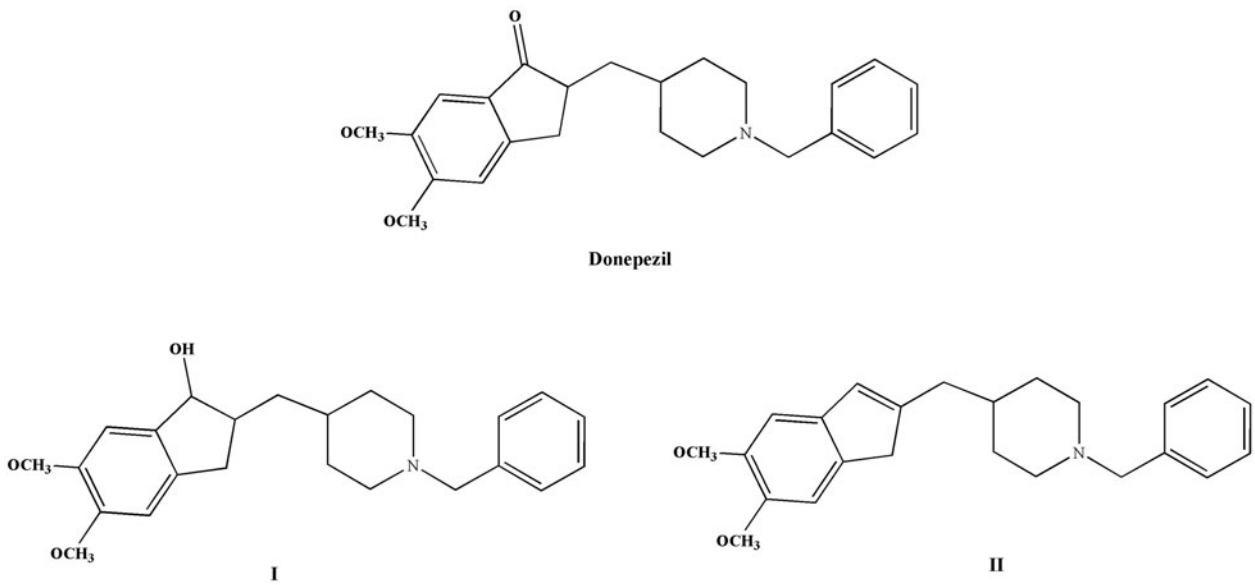

Figure 1. Structures of some AChE inhibitors: donepezil and indanol- and indene-based derivatives (**I** and **II**) reported as AChE inhibitors.

donepezil analogues. The indanone ring structure of donepezil was modified to 1H-indene to measure the possible contributions on ChE inhibition. For this purpose, we have designed a new series of secondary 5,6-dimethoxy-1H-indene-2-carboxamide derivatives containing *ortho*-, *meta*-, and *para*-substituted primary anilines and evaluated their inhibitory activities on ChEs and $A\beta_{1-42}$ aggregation and their metal chelation abilities. *In silico* studies were used to provide preliminary assessment of the potential interactions against AChE, while molecular docking studies were performed using Sybyl X 2.0 (Tripos Associates (St Louis, MO) for the most potent AChE/BuChE inhibitors.

Materials and methods

Materials

All chemical reagents, starting materials and solvents used in this study were purchased from Merck & Co. (Kenilworth, NJ), Fluka Chemical Corp. (Milwaukee, WI) and Sigma Aldrich (St. Louis, MO). The melting points were measured on an Electrothermal 9100 melting-point apparatus (Bibby Scientific Limited, Stone, UK) and are uncorrected. The NMR spectra were recorded on a Bruker FT-400(100) MHz spectrometer (Bruker corporation, Billerica, MA). Coupling constants were given in Hertz (Hz). High resolution mass spectra (HRMS) were obtained on a Waters LCT Premier XE Mass Spectrometer equipped with an ESI (+) method, also coupled to an AQUITY Ultra Performance Liquid Chromatography system (Waters Corporation, Milford, MA).

Chemistry

Synthesis procedure of 5,6-dimethoxy-indane-1-one

For the synthesis of 5,6-dimethoxy-indane-1-one, a solution of 3-(3,4-dimethoxy-phenyl)-propionic acid (4.98 g, 23.7 mmol) in dry dichloromethane (72.5 mL), N,N-dimethylformamide (1.39 mmol) and oxalyl chloride (8.03 mL, 95 mmol) were stirred at room temperature for 8 h. The reaction mixture was concentrated by rotary evaporation. A solution of crude 3-(3,4-dimethoxy-phenyl)-propionyl chloride in anhydrous dichloromethane (82 mL) was cooled with an ice bath to 0 °C and a powder of $AlCl_3$ (5.73 g, 43 mmol) was added portionwise over 30 min. The reaction was then stirred at room temperature for 3 h and cooled to 0 °C. Ice-water (85 mL) was added slowly in reaction medium to quench the excess $AlCl_3$. The layers were separated, and the aqueous phase was extracted with four portions of CH_2Cl_2 (4×85 mL). The combined organic phases were dried over Na_2SO_4, filtered and concentrated by rotary evaporation. The crude solid was dissolved in ethylacetate and treated with activated carbon, and stirred overnight. The mixture was filtered, and the filtrate was concentrated. And the target compound (5,6-dimethoxy-indane-1-one) was recrystallized from ethyl acetate and obtained as yellow solid in 75% yield.

Synthesis procedure of 5,6-dimethoxy-1-oxo-indan-2-carboxylic acid methyl ester

NaH (2.4 g, 60 mmol, 60% in mineral oil) was added slowly to the solution of 5,6-dimethoxy-indane-1-one (4 g, 20 mmol) in dimethylcarbonate (22 mL), and the suspension was refluxed at 90 °C for 2–3 h. The resulting solid was cooled to 0 °C with an ice bath. After cooling, cold water (80 mL) was added carefully. The aqueus layer was extracted with CH_2Cl_2 (3×80 mL). The combined organic extracts were dried over Na_2SO_4 and concentrated. The desired product (white solid, 60% yield) were obtained by recrystallization from ethanol[24].

General microwave-assisted synthesis of 5,6-dimethoxyindane-1-one-2-carboxamides

The suspension of 5,6-dimethoxy-1-oxo-indane-2-carboxylic acid methyl ester (1.2 mmol) and appropriate aniline (1.2 mmol) in dioxane (3 mL) was sonicated for 1 min. The reaction tube was subjected to microwave irradiation under the following conditions: power, 300 W; pressure, 15 psi; temperature, 170 °C; reaction time, 10 min. The reaction solvent was evaporated under vacuum and the crude product was purified by recrystallization with ethanol.

General synthesis of 5,6-dimethoxy-1H-indene-2-carboxamides

Appropriate 5,6-dimethoxy-1-oxo-indane-2-carboxamide (0.69 mmol) was dissolved in dry tetrahydrofuran (4 mL) and 0.4 mL methanol was added in reaction solution. $NaBH_4$ (1.035 mmol) was added portionwise at 0 °C and the mixture was stirred

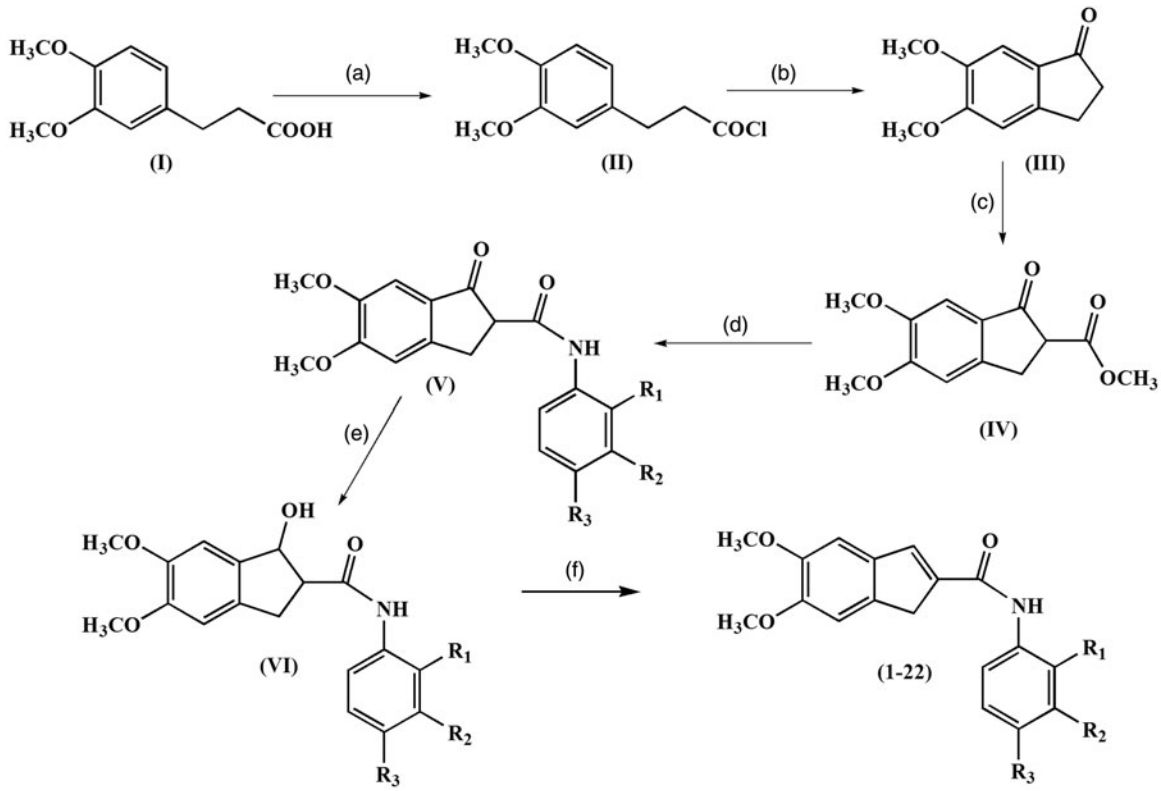

Scheme 1. Reagents and conditions: (a) oxalyl chloride, CH_2Cl_2, room temperature, 12 h; (b) $AlCl_3$, CH_2Cl_2, 0 °C, ice bath; (c) Dimethyl carbonate, NaH, 90 °C, reflux; (d) appropriate aniline, dioxane, microwave; (e) NaBH4, THF, MeOH, 2 h; (f) MeOH, PTSA, reflux, 25 min. *R_1, R_2, R_3 substituent groups at the *o*-, *m*- and *p*- positions: H, CH_3, C_2H_5, OCH_3, OC_2H_5, F, Cl and Br.

at room temperature for 2 h. The reaction solvent was evaporated and a solution of aqueous HCl (10%, 5 mL) was added in to the reaction mixture and it was stirred a few minutes. The reaction mixture was extracted with chloroform (3 × 5 mL). The combined organic layers were dried over Na_2SO_4 and concentrated. The obtained white solid product was dissolved in MeOH (4 mL) and was added catalytic amount of PTSA (*p*-toluenesulfonic acid) in reaction mixture. The reaction was refluxed for 25 min and monitored by TLC. The solvent was evaporated under reduced pressure and the resulting mixture was washed with water, and extracted with chloroform (3 × 5 mL) and dried over Na_2SO_4 and concentrated. The crude white solid was recrystallized from ethanol to obtain 5,6-dimethoxy-1H-inden-2-carboxamide derivatives. The synthesis pathway is shown in Scheme 1.

*5,6-Dimethoxy-1H-indene-2-carboxylic acid phenylamide (**1**)*

Yield 73%; m.p. 194–196 °C; λ_{maks}^{DMSO} (log ε) 336 nm (4.37). ^{1}H-NMR (400 MHz, $CDCl_3$) δ: 7.81 (s, 1H, –NH), 7.64 (d, 2H, J = 8.05 Hz, Ar-H_f), 7.52 (s, 1H, H_c), 7.33 (dd, 2H, J = 7.69 Hz, J = 7.69 Hz, Ar-H_g), 7.13–7.09 (m, 1H, Ar-H_h), 7.04 (s, 1H, Ar-H_d) 6.96 (s, 1H, Ar-H_e), 3.91 (s, 3H, Ar-OCH_3) 3.89 (s, 3H, Ar-OCH_3), 3.69 (d, 2H, H_a and H_b). ^{13}C-NMR (100 MHz, $CDCl_3$) δ: 163.14, 149.69, 148.97, 139.82, 138.31, 137.55, 137.01, 135.59, 129.27, 124.41, 120.18, 107.82, 105.94, 56.37, 56.34 and 38.56. HRMS (ESI) *m/z* $[M+H]^+$ 296.1209 (calcd for $C_{18}H_{17}NO_3$ $[M+H]^+$ 296.1208).

*5,6-Dimethoxy-1H-indene-2-carboxylic acid p-tolylamide (**2**)*

Yield 67%; m.p. 204–207 °C; λ_{maks}^{DMSO} (log ε) 336 nm (4.45). ^{1}H-NMR (400 MHz, $CDCl_3$) δ: 7.97 (s, 1H, –NH), 7.53 (d, 2H, J = 8.42 Hz, Ar-H_f), 7.49 (s, 1H, H_c), 7.09 (d, 2H, J =8.05 Hz, Ar-H_g), 6.98 (s, 1H, Ar-H_d), 6.90 (s, 1H, Ar-H_e), 3.88 (s, 3H, Ar-OCH_3) 3.85 (s, 3H, Ar-OCH_3), 3.64 (s, 2H, H_a and H_b), 2.29 (s, 3H, Ph-CH_3). ^{13}C-NMR (100 MHz, $CDCl_3$) δ: 163.23, 149.55, 148.89, 139.96, 137.53, 136.90, 135.84, 135.70, 133.96, 129.70, 120.37, 107.79, 105.90, 56.33, 56.28, 38.55 and 21.11. HRMS (ESI) *m/z* $[M+H]^+$ 310.1330 (calcd for $C_{19}H_{19}NO_3$ $[M+H]^+$ 310.1365).

*5,6-Dimethoxy-1H-indene-2-carboxylic acid (4-ethyl-phenyl)-amide (**3**)*

Yield 72%; m.p. 184–186 °C; λ_{maks}^{DMSO} (log ε) 336 nm (4.36). ^{1}H-NMR (400 MHz, $CDCl_3$) δ: 7.64 (s, 1H, –NH), 7.56 (d, 1H, J = 8.42 Hz, Ar-H_f), 7.50 (s, 1H, H_c), 7.17 (d, 2H, J = 8.42 Hz, Ar-H_g), 7.06 (s, 1H, Ar-H_d), 6.99 (s, 1H, Ar-H_e), 3.93 (s, 3H, Ar-OCH_3) 3.91 (s, 3H, Ar-OCH_3), 3.74 (s, 2H, H_a and H_b), 2.62 (q, 2H, $\underline{CH_2}$–CH_3), 1.22 (t, 3H, CH_2–$\underline{CH_3}$). ^{13}C-NMR (100 MHz, $CDCl_3$) δ: 162.95, 149.65, 148.98, 139.99, 137.49, 136.70, 135.86, 135.66, 133.96, 128.60, 120.26, 107.85, 105.94, 56.38, 56.36, 38.56, 28.55 and 15.89. HRMS (ESI) *m/z* $[M+H]^+$ 324.1518 (calcd for $C_{20}H_{21}NO_3$ $[M+H]^+$ 324.1521).

*5,6-Dimethoxy-1H-indene-2-carboxylic acid (4-methoxy-phenyl)-amide (**4**)*

Yield 60%; m.p. 205–207 °C; λ_{maks}^{DMSO} (log ε) 337 nm (4.35). ^{1}H-NMR (400 MHz, $CDCl_3$) δ: 7.77 (s, 1H, –NH), 7.53 (d, 2H, J = 9.14 Hz, Ar-H_f), 7.49 (s, 1H, Ar-H_c), 7.02 (s, 1H, Ar-H_d), 6.94 (s, 1H, Ar-H_e), 6.85 (d, 2H, J = 8.48 Hz, Ar-H_g), 3.91 (s, 3H, Ar-OCH_3) 3.88 (s, 3H, Ar-OCH_3), 3.77 (s, 3H, Ph-OCH_3), 3.66 (s, 2H, H_a and H_b). ^{13}C-NMR (100 MHz, $CDCl_3$) δ: 163.08, 156.56, 149.57, 148.93, 139.87, 137.46, 136.78, 135.69, 131.39, 122.12, 114.36, 107.82, 105.90, 56.35, 56.32, 55.68 and 38.54.

HRMS (ESI) *m/z* $[M+H]^+$ 326.1314 (calcd for $C_{19}H_{19}NO_4$ $[M+H]^+$ 326.1314).

*5,6-Dimethoxy-1H-indene-2-carboxylic acid (4-ethoxy-phenyl)-amide (**5**)*

Yield 47%; m.p. 227–229 °C; λ_{maks}^{DMSO} (log ε) 337 nm (4.35). ^{1}H-NMR (400 MHz, $CDCl_3$) δ: 7.52 (s, 1H, –NH), 7.50 (d, 2H, $J = 8.78$ Hz, Ar-H_f), 7.49 (s, 1H, Ar-H_c), 7.07 (s, 1H, Ar-H_d), 7.01 (s, 1H, Ar-H_e), 6.88 (d, 2H, $J = 9.17$ Hz, Ar-H_g), 4.02 (q, 2H, $\underline{CH_2}$–CH_3) 3.93 (s, 3H, Ar-OCH_3), 3.92 (s, 3H, Ar-OCH_3), 3.71 (s, 2H, H_a and H_b), 1.41 (t, 3H, CH_2–$\underline{CH_3}$). ^{13}C-NMR (100 MHz, $CDCl_3$) δ: 162.85, 155.98, 149.62, 148.99, 139.93, 137.43, 136.59, 135.67, 131.18, 121.95, 115.05, 107.86, 105.93, 63.92, 56.39, 56.36, 38.54 and 15.08. HRMS (ESI) *m/z* $[M+H]^+$ 340.1467 (calcd for $C_{20}H_{21}NO_4$ $[M+H]^+$ 340.1471).

*5,6-Dimethoxy-1H-indene-2-carboxylic acid (4-fluoro-phenyl)-amide (**6**)*

Yield 80%; m.p. 217–219 °C; λ_{maks}^{DMSO} (log ε) 336 nm (4.29). ^{1}H-NMR (400 MHz, $CDCl_3$) δ: 7.74 (s, 1H, –NH), 7.59 (d, 1H, $J = 8.42$ Hz, Ar-H_f), 7.51 (s, 1H, H_c), 7.04 (s, 1H, Ar-H_d), 7.00 (d, 2H, $J = 8.42$ Hz, Ar-H_g), 6.97 (s, 1H, Ar-H_e), 3.92 (s, 3H, Ar-OCH_3) 3.89 (s, 3H, Ar-OCH_3), 3.69 (s, 2H, H_a and H_b). ^{13}C-NMR (100 MHz, $CDCl_3$) δ: 163.06, 158.32, 149.78, 149.03, 139.52, 137.53, 137.12, 135.53, 134.27, 121.97, 116.00, 115.77, 107.83, 105.97, 56.37, 56.34 and 38.52. HRMS (ESI) *m/z* $[M+H]^+$ 314.1120 (calcd for $C_{18}H_{16}FNO_3$ $[M+H]^+$ 314.1114).

*5,6-Dimethoxy-1H-indene-2-carboxylic acid (4-chloro-phenyl)-amide (**7**)*

Yield 71%; m.p. 222–224 °C; λ_{maks}^{DMSO} (log ε) 338 nm (4.38). ^{1}H-NMR (400 MHz, $CDCl_3$) δ: 7.78 (s, 1H, –NH), 7.58 (d, 1H, $J = 8.78$ Hz, Ar-H_f), 7.51 (s, 1H, H_c), 7.27 (d, 2H, $J = 8.78$ Hz, Ar-H_g), 7.03 (s, 1H, Ar-H_d), 6.96 (s, 1H, Ar-H_e), 3.91 (s, 3H, Ar-OCH_3) 3.89 (s, 3H, Ar-OCH_3), 3.67 (s, 2H, H_a and H_b). ^{13}C-NMR (100 MHz, $CDCl_3$) δ: 160.08, 149.85, 149.04, 139.39, 137.59, 137.34, 136.88, 135.46, 129.32, 129.24, 121.39, 107.82, 105.99, 56.37, 56.34 and 38.51. HRMS (ESI) *m/z* $[M+H]^+$ 330.0817 (calcd for $C_{18}H_{16}ClNO_3$ $[M+H]^+$ 330.0819).

*5,6-Dimethoxy-1H-indene-2-carboxylic acid (4-bromo-phenyl)-amide (**8**)*

Yield 70%; m.p. 228–230 °C; λ_{maks}^{DMSO} (log ε) 339 nm (4.41). ^{1}H-NMR (400 MHz, $CDCl_3$) δ: 7.80 (s, 1H, –NH), 7.54 (s, 1H, H_c), 7.51 (d, 2H, J =7.68 Hz, Ar-H_f), 7.42 (d, 2H, $J = 8.78$ Hz, Ar-H_g), 7.03 (s, 1H, Ar-H_d), 6.95 (s, 1H, Ar-H_e), 3.91 (s, 3H, Ar-OCH_3) 3.88 (s, 3H, Ar-OCH_3), 3.67 (d, 2H, H_a and H_b). ^{13}C-NMR (100 MHz, $CDCl_3$) δ: 163.09, 149.85, 149.03, 139.37, 137.60, 137.40, 136.84, 135.45, 132.18, 121.72, 116.92, 107.81, 105.99, 56.37, 56.35 and 38.50. HRMS (ESI) *m/z* $[M+H]^+$ 374.0314 (calcd for $C_{18}H_{16}BrNO_3$ $[M+H]^+$ 374.0314).

*5,6-Dimethoxy-1H-indene-2-carboxylic acid m-tolylamide (**9**)*

Yield 50%; m.p. 159–161 °C; λ_{maks}^{DMSO} (log ε) 336 nm (4.42). ^{1}H-NMR (400 MHz, DMSO-d_6) δ: 9.63 (s, 1H, –NH), 7.68 (s, 1H, Ar-H_c), 7.59 (s, 1H, Ar-H_f), 7.54 (d, 1H, $J = 8.60$ Hz, Ar-H_i), 7.20 (s, 1H, Ar-H_d), 7.18–7.16 (m, 2H, Ar-H_h and Ar-H_e), 6.86 (d, 1H, $J = 7.36$ Hz, Ar-H_g), 3.80 (s, 3H, Ar-OCH_3), 3.79 (s, 3H, Ar-OCH_3), 3.68 (s, 2H, H_a and H_b), 2.29 (s, 3H, Ph-CH_3). ^{13}C-NMR (100 MHz, DMSO-d_6) δ: 163.19, 149.69, 149.14, 140.79, 139.70, 138.09, 137.77, 136.76, 135.96, 128.78, 124.34, 121.08, 117.72, 109.19, 107.29, 56.44, 56.41, 38.85 and 21.61. HRMS (ESI) *m/z* $[M+H]^+$ 310.1365 (calcd for $C_{19}H_{19}NO_3$ $[M+H]^+$ 310.1365).

*5,6-Dimethoxy-1H-indene-2-carboxylic acid (3-ethyl-phenyl)-amide (**10**)*

Yield 55%; m.p. 161–164 °C; λ_{maks}^{DMSO} (log ε) 337 nm (3.94). ^{1}H-NMR (400 MHz, DMSO-d_6) δ: 9.76 (s, 1H, –NH), 7.70 (s, 1H, Ar-H_c), 7.59 (s, 1H, Ar-H_f), 7.57 (d, 1H, $J = 9.13$ Hz, Ar-H_i), 7.21 (d, 1H, J =7.76 Hz, Ar-H_h), 7.19 (s, 1H, Ar-H_d), 7.17 (s, 1H, Ar-H_e), 6.89 (d, 1H, $J = 7.76$ Hz, Ar-H_g), 3.79 (s, 3H, Ar-OCH_3), 3.78 (s, 3H, Ar-OCH_3), 3.67 (s, 2H, H_a and H_b), 2.57 (q, 2H, $\underline{CH_2}CH_3$), 1.17 (t, 3H, $CH_2\underline{CH_3}$). ^{13}C-NMR (100 MHz, DMSO-d_6) δ: 163.38, 149.63, 149.06, 144.73, 140.85, 139.95, 137.83, 137.09, 135.94, 129.13, 123.40, 119.99, 118.07, 108.92, 107.01, 56.39 (2× Ar-OCH_3), 39.06, 29.00 and 16.24. HRMS (ESI) *m/z* $[M+H]^+$ 324.1507 (calcd for $C_{20}H_{21}NO_3$ $[M+H]^+$ 324.1521).

*5,6-Dimethoxy-1H-indene-2-carboxylic acid (3-methoxy-phenyl)-amide (**11**)*

Yield 35%; m.p. 159–162 °C; λ_{maks}^{DMSO} (log ε) 337 nm (4.33). ^{1}H-NMR (400 MHz, DMSO-d_6) δ: 9.79 (s, 1H, –NH), 7.71 (s, 1H, Ar-H_c), 7.45 (s, 1H, Ar-H_f), 7.31 (d, 1H, $J = 8.22$ Hz, Ar-H_i), 7.21 (d, 1H, $J = 8.22$ Hz, Ar-H_g), 7.19 (s, 1H, Ar-H_d), 7.18 (s, 1H, Ar-H_e), 6.62 (dd, 1H, $J = 8.22$ Hz, J=8.22 Hz, Ar-H_h), 3.79 (s, 3H, Ar-OCH_3), 3.78 (s, 3H, Ar-OCH_3), 3.73 (s, 3H, Ph-OCH_3), 3.67 (s, 2H, H_a and H_b). ^{13}C-NMR (100 MHz, DMSO-d_6) δ: 163.48, 160.07, 149.68, 149.08, 141.19, 140.75, 137.87, 137.22, 135.90, 130.00, 112.83, 109.36, 108.93, 107.04, 106.24, 56.42, 56.40 and 55.63. HRMS (ESI) *m/z* $[M+H]^+$ 326.1315 (calcd for $C_{19}H_{19}NO_4$ $[M+H]^+$ 326.1314).

*5,6-Dimethoxy-1H-indene-2-carboxylic acid (3-ethoxy-phenyl)-amide (**12**)*

Yield 45%; m.p. 167–169 °C; λ_{maks}^{DMSO} (log ε) 337 nm (4.36). ^{1}H-NMR (400 MHz, DMSO-d_6) δ: 9.76 (s, 1H, –NH), 7.70 (s, 1H, Ar-H_c), 7.44 (s, 1H, Ar-H_f), 7.29 (d, 1H, $J = 8.68$ Hz, Ar-H_i), 7.19 (d, 1H, $J = 7.76$ Hz, Ar-H_g), 7.18 (s, 1H, Ar-H_d), 7.17 (s, 1H, Ar-H_e), 6.60 (dd, 1H, $J = 7.76$ Hz, $J = 7.76$ Hz, Ar-H_h), 3.98 (q, 2H, $O\underline{CH_2}CH_3$), 3.79 (s, 3H, Ar-OCH_3), 3.78 (s, 3H, Ar-OCH_3), 3.67 (s, 2H, H_a and H_b), 1.32 (t, 3H, $OCH_2\underline{CH_3}$). ^{13}C-NMR (100 MHz, DMSO-d_6) δ: 163.47, 159.34, 149.69, 149.09, 141.16, 140.78, 137.87, 137.19, 135.91, 129.97, 112.72, 109.95, 108.94, 107.05, 106.69, 63.55, 56.42, 56.41, 39.05 and 15.37. HRMS (ESI) *m/z* $[M+H]^+$ 340.1468 (calcd for $C_{20}H_{21}NO_4$ $[M+H]^+$ 340.1471).

*5,6-Dimethoxy-1H-indene-2-carboxylic acid (3-fluoro-phenyl)-amide (**13**)*

Yield 32%; m.p. 161–164 °C; λ_{maks}^{DMSO}(log ε) 338 nm (4.39). ^{1}H-NMR (400 MHz, DMSO-d_6) δ: 10.06 (s, 1H, –NH), 8.01 (s, 1H, Ar-H_f), 7.76 (s, 1H, Ar-H_c), 7.72 (d, 1H, J=8.22 Hz, Ar-H_i), 7.31 (d, 1H, J=7.76 Hz, Ar-H_g), 7.23 (dd, 1H, J=8.21 Hz, J=8.22 Hz, Ar-H_h), 7.19 (s, 1H, Ar-H_d), 7.18 (s, 1H, Ar-H_e), 3.79 (s, 3H, Ar-OCH_3), 3.78 (s, 3H, Ar-OCH_3), 3.67 (s, 2H, H_a and H_b). ^{13}C-NMR (100 MHz, DMSO-d_6) δ: 163.66, 161.55, 149.81, 149.11, 141.75, 140.32, 137.99, 137.72, 135.79, 130.86, 130.77, 116.20, 110.11, 108.89, 107.28, 107.08, 56.40 (2× Ar-OCH_3) and 39.01. HRMS (ESI) *m/z* $[M+H]^+$ 314.1121 (calcd for $C_{18}H_{16}FNO_3$ $[M+H]^+$ 314.1114).

*5,6-Dimethoxy-1H-indene-2-carboxylic acid (3-chloro-phenyl)-amide (**14**)*

Yield 30%; m.p. 160–163 °C; λ_{maks}^{DMSO} (log ε) 339 nm (4.28). ^{1}H-NMR (400 MHz, DMSO-d_6) δ: 9.97 (s, 1H, –NH), 7.93 (s, 1H,

Ar-H_f), 7.73 (s, 1H, Ar-H_c), 7.66 (d, 1H, J=8.22 Hz, Ar-H_i), 7.33 (dd, 1H, J=8.22 Hz, J=8.22 Hz, Ar-H_h), 7.20 (s, 1H, Ar-H_d), 7.19 (s, 1H, Ar-H_e), 6.88 (d, 1H, J=7.76 Hz, Ar-H_g), 3.79 (s, 3H, Ar-OCH_3), 3.78 (s, 3H, Ar-OCH_3), 3.67 (s, 2H, H_a and H_b). ^{13}C-NMR (100 MHz, DMSO-d_6) δ: 163.64, 149.86, 149.14, 141.52, 140.27, 138.02, 137.83, 135.81, 131.60, 130.96, 123.49, 119.92, 118.85, 108.93, 107.13, 56.43, 56.41 and 39.01. HRMS (ESI) *m/z* $[M+H]^+$330.0815 (calcd for $C_{18}H_{16}ClNO_4$ $[M+H]^+$330. 0819).

*5,6-Dimethoxy-1H-indene-2-carboxylic acid (3-bromo-phenyl)-amide (**15**)*

Yield 34%; m.p. 155–157 °C; λ_{maks}^{DMSO} (log ε) 339 nm (4.29). ^{1}H-NMR (400 MHz, DMSO-d_6) δ: 9.96 (s, 1H, –NH), 8.07 (s, 1H, Ar-H_f), 7.73 (s, 1H, Ar-H_c), 7.70 (d, 1H, J=8.22 Hz, Ar-H_i), 7.29 (d, 1H, J=8.22 Hz, Ar-H_g), 7.23 (dd, 1H, J=9.59 Hz, J=8.22 Hz, Ar-H_h), 7.19 (s, 1H, Ar-H_d), 7.18 (s, 1H, Ar-H_e), 3.79 (s, 3H, Ar-OCH_3), 3.77 (s, 3H, Ar-OCH_3), 3.67 (s, 2H, H_a and H_b). ^{13}C-NMR (100 MHz, DMSO-d_6) δ: 163.59, 149.82, 149.10, 141.64, 140.23, 138.00, 137.83, 135.77, 131.26, 126.36, 122.74, 122.08, 119.20, 108.89, 107.10, 56.41, 56.39 and 39.00. HRMS (ESI) *m/z* $[M+H]^+$374.0322 (calcd for $C_{18}H_{16}BrNO_4$ $[M+H]^+$374.0314).

*5,6-Dimethoxy-1H-indene-2-carboxylic acid o-tolylamide (**16**)*

Yield 48%; m.p. 197–200 °C; λ_{maks}^{DMSO} (log ε) 329 nm (4.31). ^{1}H-NMR (400 MHz, DMSO-d_6) δ: 9.41 (s, 1H, –NH), 7.66 (s, 1H, Ar-H_c), 7.32 (d, 1H, J = 7.31 Hz, Ar-H_i), 7.26–7.21 (m, 2H, Ar-H_h and Ar-H_g), 7.19 (s, 1H, Ar-H_d), 7.18 (s, 1H, Ar-H_e), 7.12 (d, 1H, J = 6.85 Hz, Ar-H_f), 3.79 (s, 3H, Ar-OCH_3), 3.78 (s, 3H, Ar-OCH_3), 3.67 (s, 2H, H_a and H_b), 2.23 (s, 3H, Ph-CH_3). ^{13}C-NMR (100 MHz, DMSO-d_6) δ: 163.30, 149.57, 149.54, 140.63, 139.94, 137.68, 137.08, 135.99, 133.80, 130.94, 126.78, 126.61, 126.22, 108.94, 106.97, 56.39 (2× Ar-OCH_3) and 39.00, 18.59. HRMS (ESI) *m/z* $[M+H]^+$310.1360 (calcd for $C_{19}H_{19}NO_3$ $[M+H]^+$310.1365).

*5,6-Dimethoxy-1H-indene-2-carboxylic acid (2-ethyl-phenyl)-amide (**17**)*

Yield 42%; m.p. 196–200 °C; λ_{maks}^{DMSO} (log ε) 329 nm (4.21). ^{1}H-NMR (400 MHz, DMSO-d_6) δ: 9.40 (s, 1H, –NH), 7.66 (s, 1H, Ar-H_c), 7.31 (d, 1H, J = 6.39 Hz, Ar-H_i), 7.25 (dd, 1H, J = 5.94 Hz, J = 6.39 Hz, Ar-H_g), 7.19 (s, 1H, Ar-H_d), 7.18 (s, 1H, Ar-H_e), 7.16 (d, 1H, J = 8.05 Hz, Ar-H_f), 3.79 (s, 3H, Ar-OCH_3), 3.77 (s, 3H, Ar-OCH_3), 3.75 (s, 2H, H_a and H_b), 2.57 (q, 2H, $\underline{CH_2}CH_3$), 1.11 (t, 3H, $CH_2\underline{CH_3}$). ^{13}C-NMR (100 MHz, DMSO-d_6) δ: 163.67, 149.54, 149.02, 140.63, 139.94, 137.68, 136.96, 136.41, 135.98, 129.09, 127.77, 126.74, 126.60, 108.92, 106.95, 56.38 (2× Ar-OCH_3), 39.02, 24.64 and 14.75. HRMS (ESI) *m/z* $[M+H]^+$324.1526 (calcd for $C_{20}H_{21}NO_3$ $[M+H]^+$324.1521).

*5,6-Dimethoxy-1H-indene-2-carboxylic acid (2-methoxy-phenyl)-amide (**18**)*

Yield 47%; m.p. 206–209 °C; λ_{maks}^{DMSO} (log ε) 337 nm (4.26). ^{1}H-NMR (400 MHz, DMSO-d_6) δ: 8.88 (s, 1H, –NH), 7.93 (d, 1H, J = 8.22 Hz, Ar-H_i), 7.67 (s, 1H, Ar-H_c), 7.19 (s, 1H, Ar-H_d), 7.17 (s, 1H, Ar-H_e), 7.10–7.05 (m, 2H, Ar-H_g, Ar-H_h), 6.94 (d, 1H, J = 8.68 Hz, Ar-H_f), 3.85 (s, 3H, Ar-OCH_3), 3.79 (s, 3H, Ar-OCH_3), 3.77 (s, 3H, Ph-OCH_3), 3.68 (s, 2H, H_a and H_b). ^{13}C-NMR (100 MHz, DMSO-d_6) δ: 162.90, 150.83, 149.68, 149.05, 140.44, 137.79, 137.39, 135.93, 127.80, 125.39, 123.14, 120.97, 111.80, 108.93, 107.02, 56.47, 56.39, 56.36 and 38.73. HRMS (ESI) *m/z* $[M+H]^+$326.1320 (calcd for $C_{19}H_{19}NO_4$ $[M+H]^+$326.1314).

*5,6-Dimethoxy-1H-indene-2-carboxylic acid (2-ethoxy-phenyl)-amide (**19**)*

Yield 45%; m.p. 179–182 °C; λ_{maks}^{DMSO} (log ε) 338 nm (4.25). ^{1}H-NMR (400 MHz, DMSO-d_6) δ: 8.78 (s, 1H, –NH), 8.01 (d, 1H, J = 7.31 Hz, Ar-H_i), 7.64 (s, 1H, Ar-H_c), 7.20 (s, 1H, Ar-H_d), 7.19 (s, 1H, Ar-H_e), 7.06–7.05 (m, 2H, Ar-H_g and Ar-H_h), 6.91 (d, 1H, J=8.05 Hz, Ar-H_f), 4.10 (q, 2H, $O\underline{CH_2}CH_3$), 3.79 (s, 3H, Ar-OCH_3), 3.77 (s, 3H, Ar-OCH_3), 3.68 (s, 2H, H_a and H_b), 1.39 (t, 3H, $OCH_2\underline{CH_3}$). ^{13}C-NMR (100 MHz, DMSO-d_6) δ: 162.70, 149.72, 149.60, 149.05, 140.42, 137.74, 137.44, 135.89, 128.08, 125.11, 122.39, 121.01, 112.78, 108.93, 107.05, 64.72, 56.39, 56.34, 38.55 and 15.34. HRMS (ESI) *m/z* $[M+H]^+$340.1467 (calcd for $C_{20}H_{21}NO_4$ $[M+H]^+$340.1471).

*5,6-Dimethoxy-1H-indene-2-carboxylic acid (2-fluoro-phenyl)-amide (**20**)*

Yield 38%; m.p. 167–170 °C; λ_{maks}^{DMSO} (log ε) 333 nm (4.22). ^{1}H-NMR (400 MHz, DMSO-d_6) δ: 9.63 (s, 1H, –NH), 7.73 (s, 1H, Ar-H_c), 7.65 (d, 1H, J = 8.02 Hz, Ar-H_i), 7.25 (dd, 1H, J = 8.22 Hz, J = 8.22 Hz, Ar-H_h), 7.24–7.21 (m, 2H, Ar-H_f and Ar-H_g), 7.19 (s, 1H, Ar-H_d), 7.18 (s, 1H, Ar-H_e), 3.79 (s, 3H, Ar-OCH_3), 3.78 (s, 3H, Ar-OCH_3), 3.67 (s, 2H, H_a and H_b). ^{13}C-NMR (100MHz, DMSO-d_6) δ: 163.36, 149.77, 149.09, 139.90, 137.92, 135.87, 127.18, 126.99, 126.91, 126.61, 124.93, 124.89, 116.47, 116.27, 108.93, 107.10, 56.40 (2× Ar-OCH_3) and 38.89. HRMS (ESI) *m/z* $[M+H]^+$314.1121 (calcd for $C_{18}H_{16}FNO_3$ $[M+H]^+$314.1114).

*5,6-Dimethoxy-1H-indene-2-carboxylic acid (2-chloro-phenyl)-amide (**21**)*

Yield 41%; m.p. 156–159 °C; λ_{maks}^{DMSO} (log ε) 333 nm (4.24). ^{1}H-NMR (400 MHz, DMSO-d_6) δ: 9.49 (s, 1H, –NH), 7.72 (s, 1H, Ar-H_c), 7.68 (d, 1H, J = 8.22 Hz, Ar-H_i), 7.56 (dd, 1H, J = 7.76 Hz, J = 7.76 Hz, Ar-H_h), 7.34 (dd, 1H, J = 7.76 Hz, J = 7.76 Hz, Ar-H_g), 7.23 (d, 1H, J = 7.76 Hz, Ar-H_f), 7.20 (s, 1H, Ar-H_d), 7.19 (s, 1H, Ar-H_e), 3.79 (s, 3H, Ar-OCH_3), 3.78 (s, 3H, Ar-OCH_3), 3.68 (s, 2H, H_a and H_b). ^{13}C-NMR (100 MHz, DMSO-d_6) δ: 163.28, 149.79, 149.09, 139.88, 137.94, 137.90, 135.84, 135.71, 130.15, 128.87, 128.10, 127.96, 127.39, 108.92, 107.09, 56.38, 56.34 and 38.89. HRMS (ESI) *m/z* $[M+H]^+$330.0827 (calcd for $C_{18}H_{16}ClNO_3$ $[M+H]^+$330.0819).

*5,6-Dimethoxy-1H-indene-2-carboxylic acid (2-bromo-phenyl)-amide (**22**)*

Yield 45%; m.p. 173–175 °C; λ_{maks}^{DMSO} (log ε) 333 nm (4.24). ^{1}H-NMR (400 MHz, DMSO-d_6) δ: 9.44 (s, 1H, –NH), 7.72 (s, 1H, Ar-H_c), 7.68 (d, 1H, J = 8.68 Hz, Ar-H_i), 7.66 (d, 1H, J = 8.68 Hz, Ar-H_f), 7.39 (dd, 1H, J = 7.76 Hz, J = 7.76 Hz, Ar-H_h), 7.20 (s, 1H, Ar-H_d), 7.19 (s, 1H, Ar-H_e), 7.15 (d, 1H, J = 7.31 Hz, Ar-H_g), 3.79 (s, 3H, Ar-OCH_3), 3.78 (s, 3H, Ar-OCH_3), 3.68 (s, 2H, H_a and H_b). ^{13}C-NMR (100 MHz, DMSO-d_6) δ: 163.22, 149.80, 149.11, 139.93, 137.88, 137.08, 135.84 (2× Aromatic C), 133.29, 128.73, 128.34, 127.90, 126.88, 108.94, 107.11, 56.38 (2× Ar-OCH_3) and 38.87. HRMS (ESI) *m/z* $[M+H]^+$374.0325 (calcd for $C_{18}H_{16}BrNO_4$ $[M+H]^+$374.0314).

Inhibition studies on AChE and BuChE

The inhibitory activities of 5,6-dimethoxy-1H-indene-based secondary amide derivatives were evaluated against AChE (E.C. 3.1.1.7, Type VI-S, Electrophorus electricus) and BuChE (E.C. 3.1.1.8, equine serum) spectrophotometrically by the method of Ellman with slight modifications using commercially available donepezil hydrochloride as the reference compound[25]. Stock

solutions were dissolved in dimethylsulfoxide and then diluted in a 50 mM Tris buffer (pH 8.0) to provide a final concentration range. In a 96-well polystyrene photometric microplates, the assay medium in each well consisted of 50 μL of a Tris buffer, 125 μL of 3 mM 5,5-dithiobis-(2-nitrobenzoic acid) (DTNB), 25 μL of 0.2 U/mL enzyme (AChE or BuChE) and a 15 mM substrate acetylthiocholine iodide (ATCI) or butyrylthiocholine iodide (BTCI). The assay mixture containing the enzyme, buffer, DTNB and 25 μL of the inhibitor compound was preincubated for 15 min at 37 °C before the substrate was added to begin the reaction. All test compounds were prepared at seven different concentrations: 0.09, 0.195, 0.39, 0.78, 3.13, 12.5 and 50 μg/mL. The absorbance of the reaction mixture was then measured three times at 412 nm every 45 s using a microplate reader (Bio-Tek ELx800, Winooski, VT). The IC_{50} values of the compounds showing half of the maximal inhibitory concentration, the measurements and the calculations were determined with GraphPad Prism 6 (GraphPad Software, Inc., La Jolla, CA). Results were expressed as mean ± SD and all experiments were performed in triplicate.

The mechanism of AChE and BuChE inhibition

The compounds **20** and **21** were selected for kinetic measurements because they were found to be the highest inhibitory activity against BuChE and AChE, respectively. For this purpose, the rate of the enzyme activity was carried out without the inhibitor and in 5, 10 and 20 μM concentrations of the inhibitor for AChE and 5, 10 and 20 μM concentrations for BuChE using different concentration of the substrates (from 0.1 to 1.5 mM). The obtained data were used to create substrate-velocity curves, which were transformed in GraphPad Prism program to Lineweaver–Burk plots. Each experiment was performed in triplicate.

Inhibition of $A\beta_{1-42}$ self-induced aggregation

Thioflavin T (ThT)-based fluorometric assay is a well-known method for measuring the inhibition of $A\beta_{1-42}$ aggregation[26]. For this method, we selected a natural reference product, curcumin, that inhibits $A\beta_{1-42}$ aggregation[27]. ThT, Curcumin, and 1,1,1,3,3,3-Hexafluoro-2-propanol (HFIP) were purchased from Sigma Aldrich. $A\beta_{1-42}$ samples (Anaspec Inc., Fremont, CA) were dissolved in HFIP (1 mg/mL) and incubated for 24 h at room temperature. After solvent evaporation, HFIP pretreated $A\beta_{1-42}$ was resolubilized in dry DMSO to a final stock concentration of 200 μM. Stock solutions of each test compound were prepared in DMSO and diluted with sodium phosphate buffer (pH 7.4) at different concentrations ranging from 10 to 100 μM. Then, 20 μL of 25 μM $A\beta_{1-42}$ sample was added to each well for the incubation with 20 μL of test compounds in dark at 37 °C for 48 h with no agitation. After the incubation period, 160 μL of 5 μM ThT in 50 mM glycine-NaOH buffer (pH 8.0) was added to each well. Each assay was run in triplicate. Fluorescence was measured on a (Bio-Tek FLx800) with excitation and emission wavelengths of 446 and 490 nm, respectively.

Spectrophotometric measurement of metal-chelation capacity

The metal complexation capacities of the most potent cholinesterase and $A\beta_{1-42}$ inhibitors was studied for some metals such as Cu^{2+}, Fe^{2+} and Zn^{2+} in dimethylsulfoxide (DMSO) at room temperature by using a Ultraviolet-visible (UV–Vis) spectrophotometer with a wavelength ranging from 190 to 380 nm[28,29]. The UV absorption of test compounds **20** and **21**, in the absence or presence of $CuSO_4$, $FeSO_4$ and $ZnSO_4$, was recorded in a 1 cm quartz cuvette after 20 min at room temperature. The final volume of the reaction mixture was 3 mL, and the final concentrations of the test compounds and metals were 100 μM.

Molecular modeling procedure

The simulation system was built on the crystallographic structures of 1EVE and 1P0I, which were obtained from the Protein Data Bank. The molecular modelling studies were performed via Surflex-Dock in Sybyl-X 2.0 by Tripos Associates (St Louis, MO). 3D structures of compounds **20** and **21** were constructed using the Sybyl sketcher module. The structures were minimized using the Powell method until the gradient was 0.05 kcal/mol, max iterations: 1000 with the Tripos force field with the Gasteiger–Marsili charge. At the commencement of docking, all the water and ligands were removed and the random hydrogen atoms were added. Docking calculations using Surflex-Dock for 1EVE and 1P0I were performed through protomol generation by ligand. The parameters used were threshold 0.5 and bloat 0.

Result and discussion

Chemistry

5,6-Dimethoxy-1H-indene-2-carboxamide derivatives were synthesized via the pathway outlined in Scheme 1. In the first step, 3-(3,4-dimethoxy-phenyl)-propionic acid (**I**), that was used as the starting material, was converted to 3-(3,4-dimethoxy-phenyl)-propionyl chloride (**II**) in the presence of oxalyl chloride, in mixing CH_2Cl_2 at the room temperature for 12 h. In the second step, 5,6-dimethoxy-1-indanone (**III**) was occurred by a ring-closure reaction between 3-(3,4-dimethoxy-phenyl)-propionyl chloride and $AlCl_3$ as a Lewis acid. The indanone ring was then reacted with dimethylcarbonate in the presence of sodium hydride and resulted in 5,6-dimethoxy-1-oxo-indane-2-carboxylic acid methyl ester (**IV**). Microwave heating has been used to synthesis of secondary amides by direct irradiation of *para*, *meta* and *ortho*-substituted primary anilines–carboxylic acid methyl esters. The 5,6-dimethoxy-1-oxo-indane-2-carboxamide derivatives (**V**) were obtained with good yields only in a few minutes. In the next step, 5,6-dimethoxyindanone ring system was reduced to obtaine the intermediate reduction product, 1-hydroxy-5,6-dimethoxy-indane-2-carboxamide (**VI**), by using a mild reducing agent ($NaBH_4$) for 2 h in an ice bath (0 °C) with 100% yield. And in the final step, 1-hydroxy-5,6-dimethoxy-indane-2-carboxamide was refluxed with catalytic amount of p-toluenesulfonic acid (PTSA) in methanol for 2.5h to obtaine the 5,6-dimethoxy-1H-inden-2-carboxamides (**1**–**22**) as the final products, in moderate to good yields (30–80%). The structures of the compounds were confirmed by using the proton nuclear magnetic resonance (^{1}H-NMR), the carbon nuclear magnetic resonance (^{13}C-NMR) and HRMS.

In ^{1}H-NMR spectra, the resonance signals of the amide (–NH) proton appeared at δ 10.06–7.52 ppm for the compounds. The peaks for aromatic protons appeared in the range of δ 8.07–6.60 ppm. The ^{13}C-NMR spectra showed the characteristic resonance frequencies of the carbonyl signals of the secondary amide functional group in the range of 163.67–160.08 ppm. Also the aromatic carbons appeared at 161.55–105.90 ppm. Spectral data of the compounds are documented in Supplementary material.

Inhibitory activity against AChE and BuChE

The AChE and BuChE activities of all the compounds (**1**–**22**) were evaluated and compared with the anti-Alzheimer drug donepezil as the reference compound. The activities were measured *in vitro* by the spectrophotometric method developed by Ellman, with slight modifications[25]. The IC_{50} values (μM) for ChE inhibition and the selectivity indexes (SIs) of the compounds are summarized in Table 1, which displays how the compounds

Table 1. Anticholinesterase activity, inhibition of self-induced $A\beta_{1-42}$ aggregation of the compounds (**1–22**).

Compound	R^1	R^2	R^3	IC_{50} (μM)±SD§		Selectivity for BuChE‡	$A\beta_{1-42}$ aggregation inhibition¶,§ (%)	Log P‖	MR‖
				AChE*,§	BuChE†,§				
1	H	H	H	6.42 ± 1.685	1.23 ± 0.125	5.2	34.6 ± 0.1	2.85	86.89
2	CH_3	H	H	4.17 ± 0.207	1.45 ± 0.07	2.9	40.3 ± 1.4	3.34	92.78
3	C_2H_5	H	H	5.16 ± 3.158	1.48 ± 0.12	3.5	31.5 ± 2.5	3.75	97.38
4	OCH_3	H	H	6.47 ± 0.33	5.07 ± 0.103	1.3	5.4 ± 0.7	2.72	94.14
5	OC_2H_5	H	H	5.27 ± 0.127	3.78 ± 0.042	1.4	9.8 ± 1.9	3.06	98.94
6	F	H	H	3.69 ± 0.08	1.38 ± 0.012	2.7	42.5 ± 2.2	3.01	87.29
7	Cl	H	H	3.85 ± 0.141	2.8 ± 0.41	1.4	30.3 ± 3.7	3.41	91.49
8	Br	H	H	3.17 ± 0.105	2.64 ± 0.01	1.2	33.4 ± 1.1	3.68	94.58
9	H	CH_3	H	4.45 ± 0.197	2.05 ± 0.059	2.2	12.7 ± 1.3	3.34	92.78
10	H	C_2H_5	H	4.63 ± 0.007	4.9 ± 0.47	0.9	8.4 ± 2.7	3.75	97.38
11	H	OCH_3	H	4.5 ± 0.197	3.05 ± 0.112	1.5	13.8 ± 1.5	2.72	94.14
12	H	OC_2H_5	H	5.87 ± 1.332	2.41 ± 0.19	2.4	22.6 ± 2.7	3.06	98.94
13	H	F	H	2.86 ± 0.172	2.23 ± 0.121	1.3	26.9 ± 1.0	3.01	87.29
14	H	Cl	H	2.29 ± 0.574	3.49 ± 0.068	0.7	10.1 ± 2.8	3.41	91.49
15	H	Br	H	4.34 ± 0.10	5.57 ± 0.27	0.8	3.8 ± 3.1	3.68	94.58
16	H	H	CH_3	3.51 ± 0.022	1.28 ± 0.059	2.7	46.4 ± 4.0	3.34	92.78
17	H	H	C_2H_5	3.50 ± 3.568	1.72 ± 0.13	2.0	37.6 ± 0.3	3.75	97.38
18	H	H	OCH_3	3.95 ± 0.06	3.71 ± 0.125	1.1	14.8 ± 2.7	2.72	94.14
19	H	H	OC_2H_5	4.87 ± 0.038	4.32 ± 0.072	1.1	11.3 ± 3.1	3.06	98.94
20	H	H	F	2.33 ± 0.021	1.08 ± 0.011	2.2	50.3 ± 2.4	3.01	87.29
21	H	H	Cl	1.33 ± 0.062	1.27 ± 0.032	1.0	45.7 ± 3.5	3.41	91.49
22	H	H	Br	3.02 ± 0.072	1.09 ± 0.31	2.8	48.2 ± 0.8	3.68	94.58
Donepezil				0.042 ± 0.041	0.54 ± 0.017	0.1			
Curcumin							42.3 ± 2.6		

*50% Inhibitory concentration of AChE.
†50% Inhibitory concentration of BuChE.
‡Selectivity for BuChE = IC_{50} (AChE)/IC_{50} (BuChE).
¶Inhibition of self-induced $A\beta_{1-42}$ aggregation (25 μM) by tested inhibitors (25 μM).
§Values are expressed as mean ± standart error of the mean of three independent experiments and each performed in triplicate (SD = standart deviation).
‖Calculated by ChemDraw 2015.
MR: Molar Refractivity.

(**1–22**) clearly showed moderate to good potency and similar inhibitory activity against both ChEs at micromolar concentrations. The synthesized compounds exhibited inhibitory activities against AChE, with IC_{50} values ranging from 1.33 to 6.47 μM. Generally, most compounds were found to be similarly effective inhibitors of both ChEs, with low SIs.

Among them, *meta*- and *ortho*-chloro-substituted analogues (14 and 21) displayed the highest AChE inhibition, with IC_{50} values of 2.29 and 1.33 μM, respectively. The other potent AChE inhibitors, **13** and **20** (*meta*- and *ortho*-fluoro analogues), showed similar activity, with IC_{50} values of 2.86 and 2.33 μM, respectively. The comparison of non-substituted compound 1 and the other substituted compounds demonstrated that substitution of any groups, except the p-methoxy substitution, at the *ortho*, *meta* and *para* positions of the phenyl ring increased anti-AChE activity between 1.09 and 4.82 times. The results indicated that substitution at any position on the phenyl ring makes a significant contribution to anti-AChE activity. Specifically, substituting the *fluorine* and *chlorine* groups at the *meta* and *ortho* positions of the phenyl ring appeared to have a crucial effect on AChE inhibition. This positive contribution might be sourced from the high electronegativity of the halogen atoms.

The IC_{50} values of compounds **1–22** showed that all compounds were good BuChE inhibitors (1.08–5.57 μM). Compounds **1** (non-substituted), **20** (*p-fluoro*-substituted), and **22** (*p-chloro*-substituted) exhibited the most powerful effects on BuChE inhibition in series, with IC_{50} values of 1.23, 1.08 and 1.09 μM and SIs of 5.2, 2.2 and 2.8, respectively (Table 1). According to the anti-BuChE results, the electron-donating groups CH_3, C_2H_5, OCH_3 and OC_2H_5, except compound **10**, at all positions (*o*-, *m*- and *p*-) on the phenyl ring provided more beneficial effects on BuChE than on AChE inhibitory activities. In these compounds, *para*- and *meta*-CH_3-substituted compounds **16** and **9** showed the most significant BuChE inhibition. The positive effects of the electron-withdrawing atoms (F, Cl and Br) were seen in BuChE inhibition, as they were with AChE inhibition. It can be stated that the AChE inhibition mechanism of the synthesized compounds depends highly on the electronegative properties of the substituent groups. However, based on the BuChE inhibition results, not only electronegativity but also hydrophobic or electrostatic interactions may be responsible for BuChE inhibition of these compounds. Conversely, in the overall evaluation of the results, no statistically significant correlation was found between the calculated LogP and molar refractivity values of the synthesized compounds and either of their ChE inhibition activities (Table 1). In the series, the most potent BuChE (**20**) and AChE (**21**) inhibitors were selected for kinetic analysis to investigate the type of inhibition.

Kinetic study of AChE and BuChE

For deep understanding of the mechanism of inhibition, we choosed the most potent ChE inhibitors, **20** and **21**, for kinetic studies. The steady-state inhibition data of the compounds for both ChEs are shown in Figure 2. Kinetic analysis of the Lineweaver–Burk plots of AChE inhibitory activity showed that there was an increasing slope and an increasing intercept at higher concentrations. The result indicates mixed-type inhibition mechanism as the result of binding to both active sites (CAS and PAS) of AChE for the compound **21**. The kinetic study of compound **20** on BuChE inhibitory activity showed that lines crossing the *x*-axis in the same point (unchanged K_m) and decreased V_{max} with

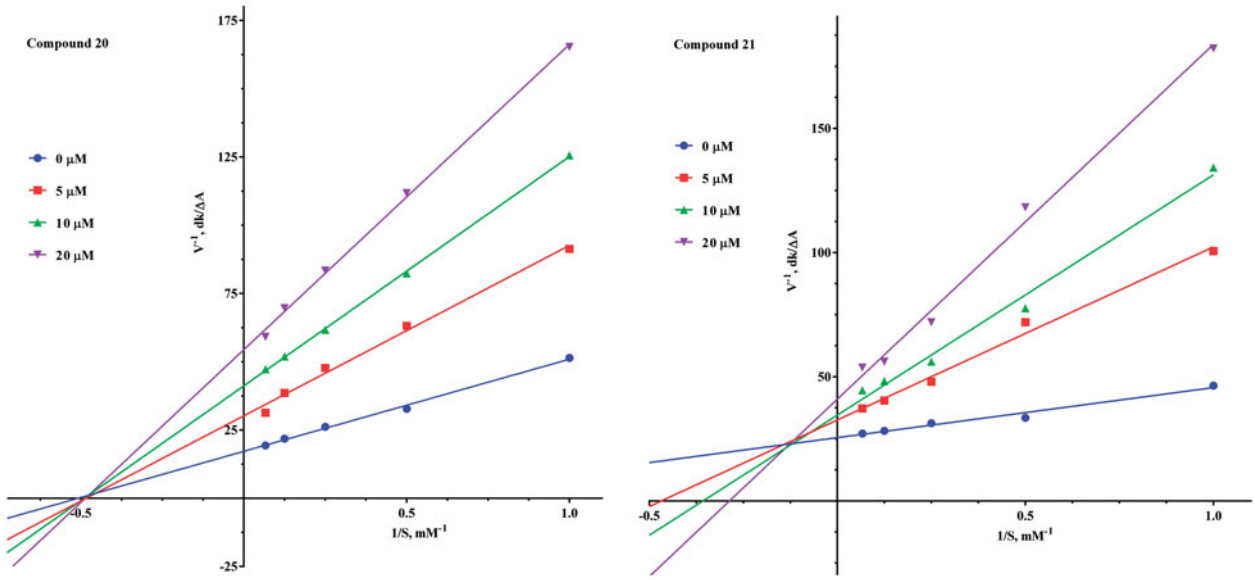

Figure 2. Lineweaver–Burk plots of inhibition kinetics of the compounds **20** and **21**.

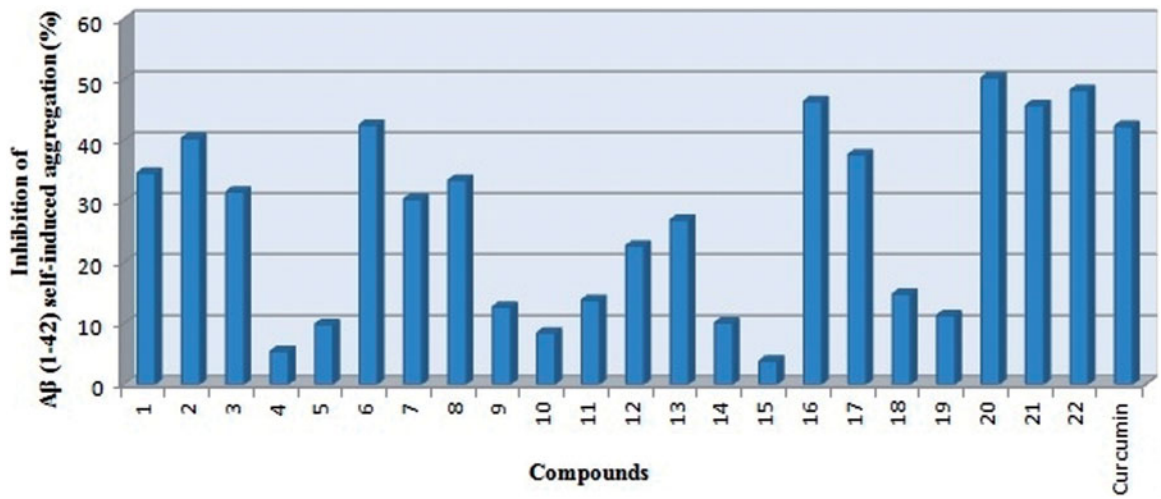

Figure 3. Inhibition of self-induced $A\beta_{1-42}$ aggregation by the test compounds and reference curcumin at concentration 25 µM.

increasing inhibitor concentrations. This result indicates that 5,6-dimethoxy-1H-indene-2-carboxamide derivatives exhibit non-competitive inhibition mechanism on BuChE.

Inhibition of $A\beta_{1-42}$ self-induced aggregation

In order to investigate the inhibition of $A\beta_{1-42}$ aggregation, a thioflavin T (ThT)-based fluorometric assay was performed[26]. Curcumin, known to be a natural product that inhibits self-induced Aβ aggregation, was used as the reference compound[30,31]. The effects on $A\beta_{1-42}$ peptide aggregation of the compounds at a concentration of 25 µM are summarized in Table 1 and Figure 3. In the ThT assay, the inhibition results showed that some of the compounds prevented $A\beta_{1-42}$ peptide aggregation with different inhibition values (3.8–55.3%). The most potent AChE inhibitors (**16**, **20** and **22**) exhibited good $A\beta_{1-42}$ inhibition potencies with respective inhibition ratios of 46.4, 50.3 and 48.2%, which are higher than curcumin's inhibition ratio (42.3%).

Studies of metal chelating effect

High levels of metal accumulation are frequently encountered in the brains of AD patients. Additionally, studies have postulated that chelation of some biometal ions (Cu^{2+}, Fe^{2+} and Zn^{2+}) might promote beneficial results in AD patients, so the chelation abilities for biometals of the most potent BuChE inhibitor (**20**) were determined by use of a spectrophotometer. The UV absorption of the compounds in dimethyl sulfoxide changed with the titration of $CuSO_4$, $FeSO_4$, and $ZnSO_4$. Compound **20** (Figure 4) showed decreased absorption peaks after adding with all metal ions used. Alterations in the absorption intensity, after adding $CuSO_4$, $FeSO_4$ and $ZnSO_4$, indicated the formation of biometal complexes for compound **20**.

In silico docking studies

The most potent ChE inhibitors are docked at the binding site of acetyl- and butyrylcholinesterase enzymes, we performed molecular modeling studies by utilizing the surflex-dock simulation program. According to the simulation results, the most potent AChE inhibitor **21** displayed multiple binding patterns with Torpedo californica (TcAChE) (Figure 5). In the 1EVE-**21** complex, all structural main moieties (5,6-dimethoxy-indanone, carboxamide and phenyl ring) occupied the CAS and PAS of enzyme and dominated several hydrogen bondings with residues Tyr130, Tyr121, Gly117 and π–π stacking interactions with residues Phe330 and Tyr334. The aromatic OCH_3 groups of the

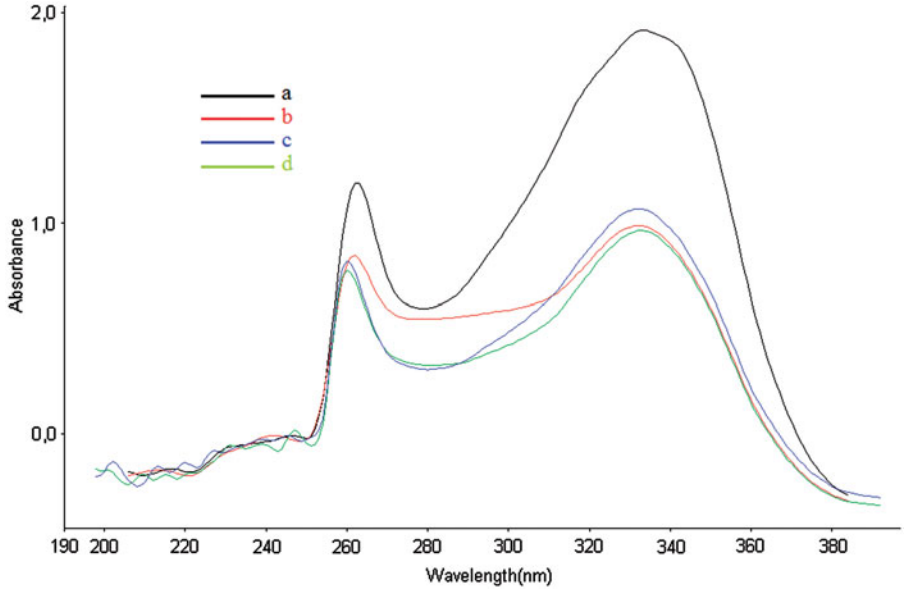

Figure 4. (a) UV absorption spectra of compound **20** (100 μM in DMSO) alone, (b) UV absorption spectra of the mixture compound **20** (100 μM) and $CuSO_4$ (100 μM), (c) UV absorption spectra of the mixture compound **20** (100 μM) and $FeSO_4$ (100 μM) and (d) UV absorption spectra of the mixture compound **20** (100 μM) and $ZnSO_4$ (100 μM).

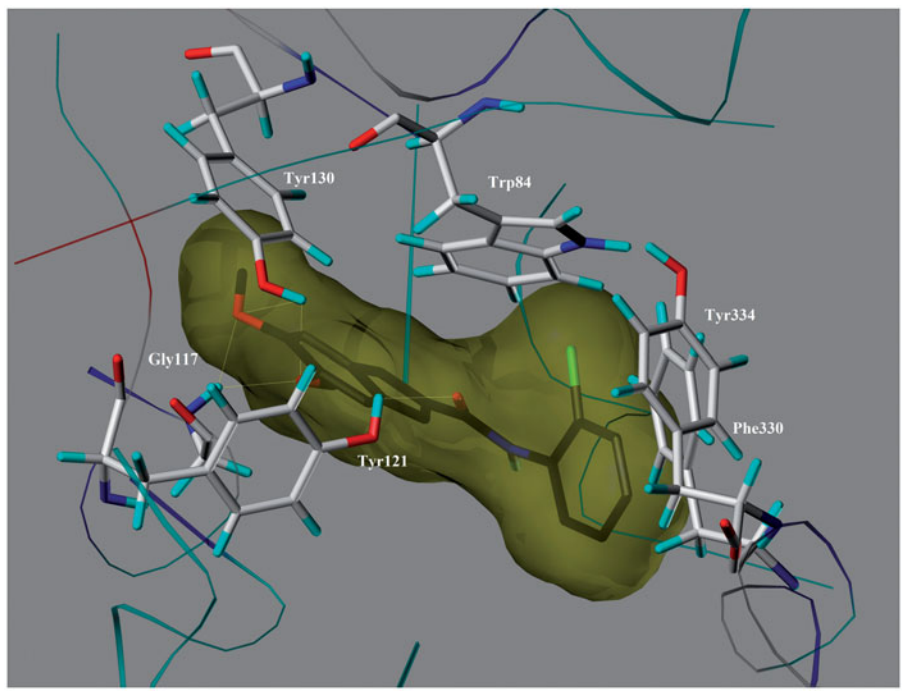

Figure 5. 3D representation of the binding mode of the most potent inhibitor **21** at the active sites of AChE.

compound **21** exhibited two hydrogen bond interactions with OH group of Tyr130 residue in CAS (distances 1.94 and 2.75 Å). The other hydrogen bonding interactions occurred between two methoxy groups of ligand **21** and NH group of Gly117 residue in oxyanion hole within the distances 1.95 and 2.68 Å. Also ligand **21** created π–π stacking interaction with indole moiety of Trp84 in CAS (distance 3.8–4.7 Å). In peripheric anionic site of 1-EVE, the C=O group of amide moiety is bridged to phenolic OH group of Tyr121 residue via hydrogen bonding (2.71 Å). In the complex, 2-chlorophenyl ring is stacked against Phe330 and Tyr334, located at the PAS. A π–π stacking interaction occurred between the phenyl group of Tyr334 residue and 2-fluorophenyl ring (2.97–2.99 Å). The simulation study of compound **21–1EVE** complex has illuminated for its potent AChE inhibitory activity and mixed-type inhibition.

On the other hand, the most potent BuChE inhibitor **20**, showed many hydrogen bonds with Thr120, Ala277, Asn68, Asn289 and Gln119 residues of Human butyrylcholinesterase enzyme (1P0I) (Figure 6). Two hydrogen bond interactions occurred between the C=O group of ligand **20** and the NH groups of Asn289 (2.43 Å) and Gln119 (1.90 Å). The OCH_3 group in position six of the indanone ring of the ligand **20** occurred a hydrogen bond with phenolic OH group of Thr120 (2.63 Å) in PAS of HuBuChE. In peripheric anionic site of 1P0I, fluorine atom at the *ortho* position on phenyl ring created a hydrogen bond with NH group of Ala277 residue (2.30 Å) and NH group of Asn68 residue (2.33 Å). These several hydrogen bonding interactions supports high anti-BuChE activity of this compound.

Conclusion

In this study, a new series of 5,6-dimethoxy-1H-indene-2-carboxamide derivatives (**1**–**22**) was developed. This study originated with an effective anti-Alzheimer drug, donepezil, which is a selective AChE inhibitor with very poor Aβ anti-aggregation activity. The aim of this research was to obtain new

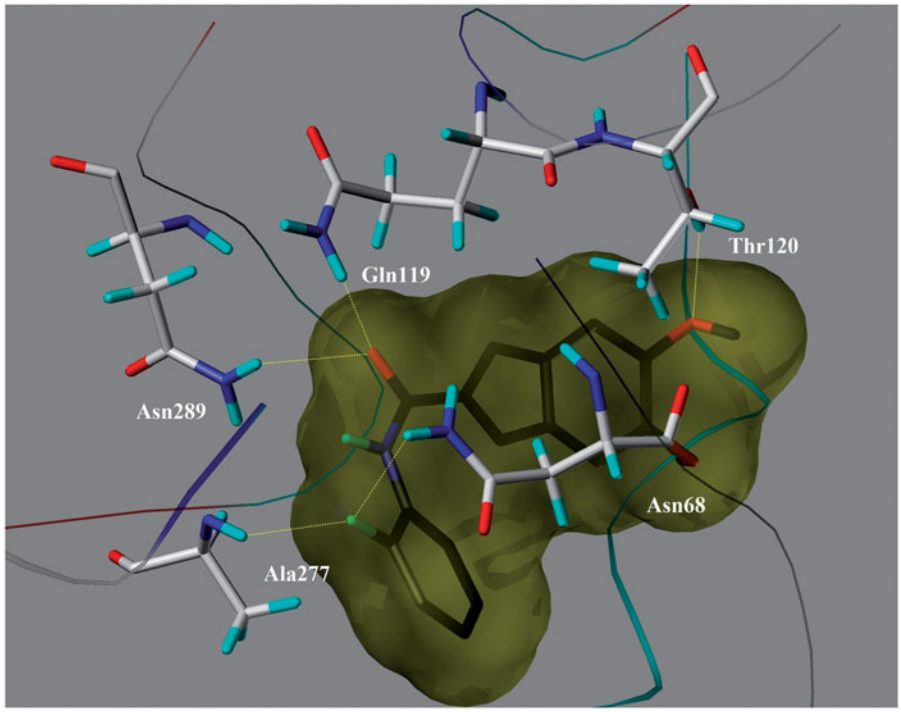

Figure 6. 3D representation of the binding mode of the most potent inhibitor **20** at the active sites of BuChE.

analogues of donepezil that are improved in their ChE and amyloid inhibition activities. Therefore, one of the pharmacophore moieties (5,6-dimethoxyindanone) of donepezil was modified to 5,6-dimethoxy-1H-indene; a secondary amide bridge was constructed with different substituted primary anilines to obtain 1H-inden-based secondary carboxamide analogues to measure the possible effects on ChE inhibition. Among the analogues, compound **20** (IC_{50}=1.08 ± 0.011 μM, BuChE) and compound **21** (IC_{50} = 1.33 ± 0.062 μM, AChE) were found to be the most effective inhibitors for ChE inhibition. The ChE inhibition results show that the structure of 5,6-dimethoxy-1H-indene-2-carboxamide derivatives makes a more positive contribution to BuChE inhibition than to AChE inhibition. At the same time, the most potent BuChE inhibitor, compound **20**, was found to be the most potent inhibitor for $A\beta_{1-42}$ aggregation (50.3%±2.4 at 25μM). Docking simulations also supported the cholinesterase inhibition study of the most potent BuChE inhibitor (**20**), which exhibited many hydrogen-bonding interactions with amino acid residues in the PAS of BuChE. Further studies to synthesize 5,6-dimethoxy-1H-indene-based tertiary amide analogues and explore their anti-Alzheimer activities are in progress.

Acknowledgements

This research work was supported by Ataturk University Research Fund (Project No: 2015/326), Turkey. The measurement of cholinesterase inhibitions was performed at the Faculty of Pharmacy and Department of Pharmaceutical Chemistry, University of Ataturk, Turkey, under the supervision of Prof. Dr. H. Inci Gul.

Declaration of interest

The authors have declared no conflicts of interest with the presented data from this article.

References

1. Hardy J, Bogdanovic N, Winblad B, et al. Pathways to Alzheimer's disease. J Intern Med 2014;275:296–303.
2. Samadi A, Estrada M, Pérez C, et al. Pyridonepezils, new dual AChE inhibitors as potential drugs for the treatment of Alzheimer's disease: synthesis, biological assessment, and molecular modeling. Eur J Med Chem 2012;57:296–301.
3. Sugimoto H, Ogura H, Arai Y, et al. Research and development of donepezil hydrochloride, a new type of acetylcholinesterase inhibitor. Jpn J Pharmacol 2002;89:7–20.
4. Akasofu S, Kimura M, Kosasa I, et al. Study of neuroprotection of donepezil, a therapy for Alzheimer's disease. Chem Biol Interact 2008;175:222–6.
5. Dumas JA, Newhouse PA. The cholinergic hypothesis of cognitive aging revisited again: cholinergic functional compensation. Pharmacol Biochem Behav 2011;99:254–61.
6. Tai HC, Serrano-Pozo A, Hashimoto T, et al. The synaptic accumulation of hyperphosphorylated tau oligomers in Alzheimer disease is associated with dysfunction of the ubiquitin-proteasome system. Am J Pathol 2012;181:1426–35.
7. Li B, Stribley JA, Ticu A, et al. Abundant tissue butyrylcholinesterase and its possible function in the acetylcholinesterase knockout mouse. J Neurochem 2000;75:1320–31.
8. Mesulam MM, Guillozet A, Show P, et al. Acetylcholinesterase knockouts establish central cholinergic pathways and can use butyrylcholinesterase to hydrolyze acetylcholine. Neuroscience 2002;110:627–39.
9. Darvesh S, Hopkins DA, Geula C. Neurobiology of butyrylcholinesterase. Nat Rev Neurosci 2003;4:131–8.
10. Fernández-Bachiller MI, Pérez C, González-Muñoz GC, et al. Novel tacrine-8-hydroxyquinoline hybrids as multifunctional agents for the treatment of Alzheimer's disease, with neuroprotective, cholinergic, antioxidant, and copper-complexing properties. J Med Chem 2010;53:4927–37.
11. Galdeano C, Viayna E, Arroyo P, et al. Structural determinants of the multifunctional profile of dual binding site acetylcholinesterase inhibitors as anti-Alzheimer agents. Curr Pharm Des 2010;16:2816–36.
12. Yankner BA, Dawes LR, Fisher S, et al. Neurotoxicity of a fragment of the amyloid precursor associated with Alzheimer's disease. Science 1989;245:417–20.
13. He Y, Yao PF, Chen SB, et al. Synthesis and evaluation of 7,8-dehydrorutaecarpine derivatives as potential multifunctional agents for the treatment of Alzheimer's disease. Eur J Med Chem 2013;63:299–312.
14. Bush AI. Drug development based on the metals hypothesis of Alzheimer's disease. J Alzheimers Dis 2008;15:223–40.
15. Dong J, Atwood CS, Anderson VE, et al. Metal binding and oxidation of amyloid-beta within isolated senile plaque cores: Raman microscopic evidence. Biochemistry 2003;42:2768–73.

16. Opazo C, Huang X, Cherny RA, et al. Metalloenzyme-like activity of Alzheimer's disease beta-amyloid. Cu-dependent catalytic conversion of dopamine, cholesterol, and biological reducing agents to neurotoxic H(2)O(2). J Biol Chem 2002;277:40302–8.
17. Hansen RA, Gartlehner G, Webb AP, et al. Efficacy and safety of donepezil, galantamine, and rivastigmine for the treatment of Alzheimer's disease: a systematic review and meta-analysis. Clin Interv Aging 2008;3:211–25.
18. FDA Approves Expanded Use of Treatment for Patients with Severe Alzheimer's Disease [press release]. U.S. Food and Drug Administration; 2006.
19. Kasap Z, Yerdelen KO, Koca M, Anil B. Synthesis, docking, metal chelating and biological activity of new oxalamide analogues for Alzheimer disease. Lat Am J Pharm 2015;34:924–33.
20. Koca M, Yerdelen KO, Anil B, Kasap Z. Microwave assisted synthesis, molecular docking, and cholinesterase inhibitory activities of new ethanediamide and 2-butenediamide analogues. Chem Pharm Bull 2015;63:210–17.
21. Yerdelen KO, Gul HI. Synthesis and anticholinesterase activity of fumaramide derivatives. Med Chem Res 2013;22:4920–9.
22. Yerdelen KO, Koca M, Kasap Z, Anil B. Preparation, anticholinesterase activity, and docking study of new 2-butenediamide and oxalamide derivatives. J Enzyme Inhib Med Chem 2015;30:671–8.
23. Yerdelen KO, Tosun E. Synthesis, docking and biological evaluation of oxamide and fumaramide analogs as potential AChE and BuChE inhibitors. Med Chem Res 2015;24:588–602.
24. Fukushi H, Mabuchi H, Itoh K, et al. Synthesis and platelet-activating factor (PAF)-antagonistic activities of 1,4-disubstituted piperazine derivatives. Chem Pharm Bull 1994;42:541–50.
25. Ellman GL, Courtney D, Andies V, Featherstone RM. A new and rapid colorimetric determination of acetylcholinesterase activity. Biochem Pharmacol 1961;7:88–95.
26. Rosini M, Simoni E, Bartolini M, et al. Inhibition of acetylcholinesterase, beta-amyloid aggregation, and NMDA receptors in Alzheimer's disease: a promising direction for the multi-target-directed ligands gold rush. J Med Chem 2008;51:4381–4.
27. Yang F, Lim GP, Begum AN, et al. Curcumin inhibits formation of amyloid beta oligomers and fibrils, binds plaques, and reduces amyloid *in vivo*. J Biol Chem 2005;280:5892–901.
28. Huang W, Lv D, Yu H, et al. Dual-target-directed 1,3-diphenylurea derivatives: BACE 1 inhibitor and metal chelator against Alzheimer's disease. Bioorg Med Chem 2010;18:5610–15.
29. Joseph R, Ramanujam B, Acharya A, et al. Experimental and computational studies of selective recognition of Hg2+ by amide linked lower rim 1,3-dibenzimidazole derivative of calix[4]arene: species characterization in solution and that in the isolated complex, including the delineation of the nanostructures. J Org Chem 2008;73:5745–58.
30. Endo H, Nikaido Y, Nakadate M, et al. Structure activity relationship study of curcumin analogues toward the amyloid-beta aggregation inhibitor. Bioorg Med Chem Lett 2014;24:5621–6.
31. Prinz M, Parlar S, Bayraktar G, et al. 1,4-Substituted 4-(1H)-pyridylene-hydrazone-type inhibitors of AChE, BuChE, and amyloid-β aggregation crossing the blood-brain barrier. Eur J Pharm Sci 2013;49:603–13.

Supplementary material available online